

of the straight section of the nozzle. The laminar boundary-layer displacement thickness, including the effects of compressibility and deceleration of the freestreams, was calculated from the results presented by Moore.<sup>5</sup> The turbulent boundary-layer displacement thickness was calculated for an incompressible fluid. However, the effects of compressibility were estimated from the work of Cope<sup>1</sup> and were found to have a relatively small effect on  $\delta^*/d$  in the range of conditions tested. In the experiments performed, the Reynolds numbers based on the equivalent flat plate length ranged from 0.5 to  $2.5 \times 10^6$ . The experimentally determined effective contraction ratios are plotted in Figs. 3a and 3b for laminar and turbulent boundary-layer growth on the equivalent flat plate, respectively. The effect of the assumption on the equivalent flat-plate length for the converging section of the nozzle is also indicated for several points in Fig. 3 by assuming the length equal to  $\frac{1}{3}$  and  $\frac{2}{3}$  of the major axis.

### Conclusions

For the range of conditions covered, the experimental results indicate that the pressure variation inside the vessel can be closely approximated by assuming that the flow is one-dimensional and quasi-steady within the nozzle and that the discharge area is equal to the physical area of the nozzle.

### References

- <sup>1</sup> Cope, W., *Modern Developments in Fluid Dynamics, High Speed Flow*, edited by L. Howarth (Oxford University Press, London, 1953), Vol. 1, pp. 456-462.
- <sup>2</sup> Hall, G. W., "Application of boundary layer theory to explain some nozzle and venturi peculiarities," *Proc. Inst. Mech. Engrs.* **173**, 837-870 (1959).
- <sup>3</sup> de Haller, P., "On a graphical method of gas dynamics," *Sulzer Tech. Rev.* **1**, 6-24 (1945).
- <sup>4</sup> Kestin, J. and Glass, J. S., "The rapid discharge of a gas from vessels," *Aircraft Eng.* **23**, 300-304 (1951).
- <sup>5</sup> Moore, F. K., "Unsteady laminar boundary layer flow," NACA TN 2471 (1951).
- <sup>6</sup> Progelhof, R. C. and Owczarek, J. A., "The rapid discharge of a gas from a cylindrical vessel through an orifice," *Am. Soc. Mech. Engrs. Paper 63-WA-10* (1963).
- <sup>7</sup> Schlichting, H., *Boundary Layer Theory* (McGraw Hill Book Co. Inc., New York, 1960), Chap. 7, 15, 21.
- <sup>8</sup> Simmons, F. G., "Analytical determination of the discharge coefficients of flow nozzles," NACA TN 3447 (1955).

## Far Infrared Radiation Model of the Earth

ROBERT A. MCGEE\*

General Electric Company, Utica, N. Y.

### Introduction

MANY space vehicles contain equipment to sense infrared radiation from the earth. The spectral region from 7 to 13  $\mu$ , in which the atmosphere is quite transparent, has been very popular for such equipment. At wavelengths below 2  $\mu$ , reflection of sunlight becomes a problem, and at longer wavelengths the choice of detectors and optical materials is quite limited. Germanium has been a common choice of optical material because of its high transmission in the 3- to 16- $\mu$  region and its desirable mechanical properties, and thermistor bolometers have been favored as detectors.<sup>4</sup> This combination lends itself to equipments using the 7- to 13- $\mu$  atmospheric

Presented at the IAS National Summer Meeting, Los Angeles, Calif., June 19-22, 1962; revision received July 18, 1963.

\* Engineer, Light Military Electronics Department.

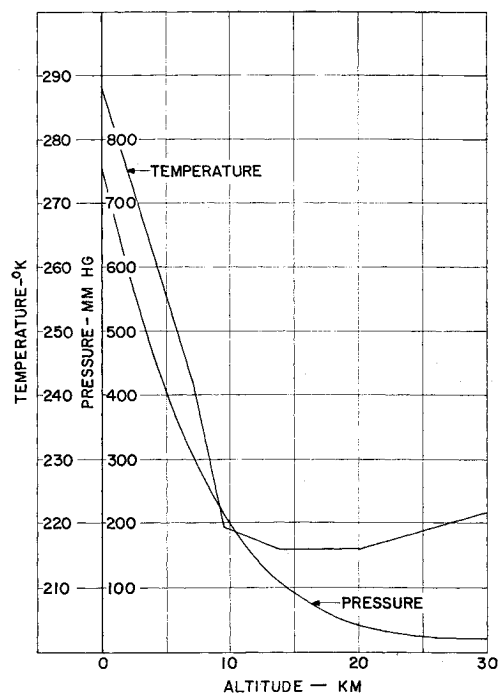


Fig. 1 Temperature and pressure profiles.

window. Recent experiments, such as the Tiros radiation experiments, however, have indicated that the radiation from the earth is highly variable in this spectral region. As a result, a study has been undertaken to determine the cause and to predict the types of variation to be expected. An analytical model was developed, and the results predicted by this model have been compared with data from the Tiros radiation experiments.

### Description of Model

The earth's atmosphere is composed of a number of gases, each of which selectively absorbs radiation transmitted through it. The absorption through any gas is a function of the amount of gas present, its temperature and pressure, and the wavelength of the transmitted radiation. The constituents that absorb infrared radiation appreciably are water vapor, carbon dioxide, ozone, and nitrous oxide. Once the amount of each constituent in a given path has been determined, the total transmission through the path as a function of wavelength may be found. The mathematical procedure

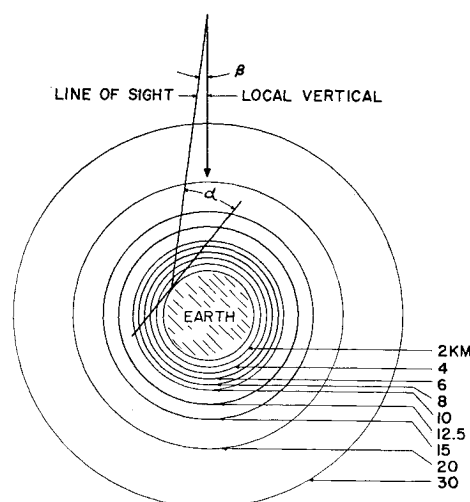


Fig. 2 Physical model and geometry.

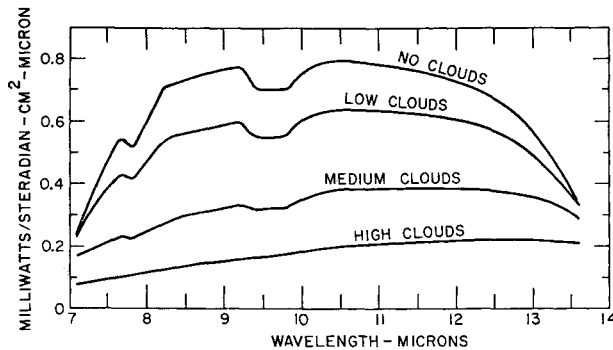


Fig. 3 Spectral radiance at nadir; ARDC atmosphere.

used in this study is reported in Ref. 1. A 1959 ARDC model atmosphere was assumed, and its parameters are shown in Fig. 1.

Figure 2 illustrates the physical model chosen for this study.<sup>2</sup> The atmosphere has been stratified into nine layers, and the earth and each layer have been assigned a temperature and pressure according to the chosen profile. Each layer has been assumed to be uniform and homogeneous. When clouds are assumed to be present, they are assigned the temperature at the altitude of the top of the cloud. It has been assumed that a cloud will absorb all radiation emanating from below and will emit as a blackbody radiator at its assigned temperature. Clouds have been assigned at altitudes of 2, 6, and 10 km. Water vapor concentration is assumed to be such as to produce a relative humidity of 100% up to the tropopause and a constant mixing ratio at higher altitudes. Ozone, CO<sub>2</sub>, and N<sub>2</sub>O distributions are those given by Altshuler.<sup>3</sup>

### Results

To provide a presentation of results which is independent of the altitude of the observer, the geometry shown in Fig. 2 has been employed. The angle  $\alpha$  is between the line of sight and the tangent to a spherical earth. When the line of sight does not intersect the earth, the altitude of its closest approach to the earth ( $h$ ) is used as a parameter. These are converted easily to the nadir angle ( $\beta$ ) of the line of sight by the relationship

$$\sin \beta = [R_e / (R_e + H)] \cos \alpha \quad (1)$$

for the case where the line of sight intersects the earth. The radius of the earth is  $R_e$ , and  $H$  is the observer altitude. For the case where the line of sight does not intersect the earth,

$$\sin \beta = (R_e + h) / (R_e + H) \quad (2)$$

Figure 3 is a typical set of results for the ARDC model atmosphere. Here, the observer is looking straight down at the center of the earth ( $\alpha = 90^\circ$ ). Absorption due to water

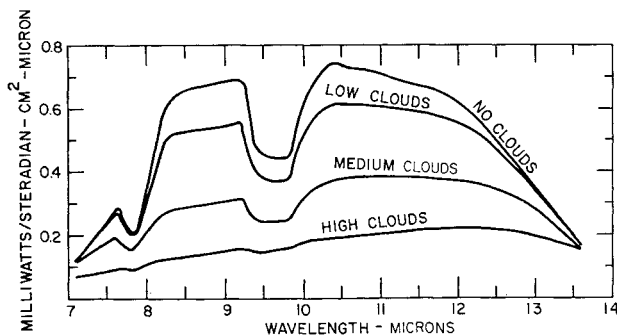
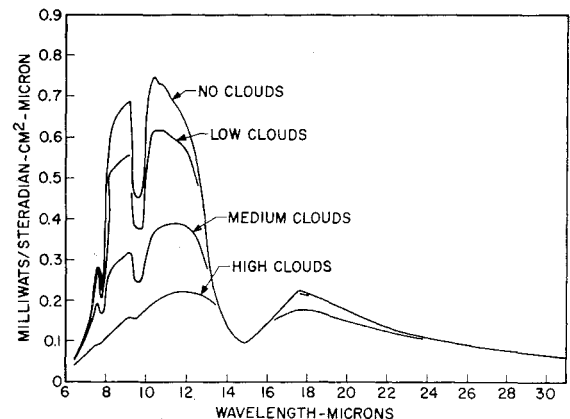


Fig. 4 Spectral radiance at horizon; ARDC atmosphere.

vapor, ozone, and carbon dioxide is clearly seen. It can be seen that the effect of clouds appearing in the field of view is to reduce the radiance to a value as small as one-quarter of the maximum value, depending on cloud altitude and temperature. Figure 4 illustrates the situation when looking at the earth's horizon ( $\alpha = 0$ ). Greater absorption due to the longer optical path of the atmosphere is evident. However, the magnitude of the cloud effect is virtually unchanged.

Another interesting effect is the tendency of all of the curves to meet between 13 and 14  $\mu$ . This is because carbon dioxide absorption makes the atmosphere very opaque, and most of the observed radiation emanates from near the top of the atmosphere. Therefore, the appearance of a cloud, which cuts off radiation from the warmer regions below, has little effect on the observed radiance. As a result, the analysis was extended to 30  $\mu$ , and a typical curve including the 6- to 30- $\mu$  region ( $\alpha = 0$ ) is shown in Fig. 5. Any of these curves may be integrated numerically to present the total radiance in a given spectral region.

Finally, a comparison has been made of the forementioned results with data from the Tiros II radiometer channel 2, which covers the 8- to 13- $\mu$  band. The equivalent blackbody temperatures predicted by the model vary from 200°K when high clouds are present to 280°K when there are no clouds.


 Fig. 5 Spectral radiance at horizon, 6 to 30  $\mu$ .

These compare reasonably well with Tiros II data taken over the United States, which show variations from about 205°K off the coast of Florida on July 22, 1961, to readings of about 277°K, which are quite common. The 205°K incident occurred in the vicinity of high clouds accompanying hurricane Anna. Erratic readings between 225° and 285°K are quite common near scattered or broken clouds, as predicted by the model. Thus, it is felt that the model may be used to obtain a reasonably good estimate of the types of variations to be expected and the limits of their magnitudes. A recent report by Block and Lovett<sup>5</sup> presents some measurements taken from on-board a Discoverer satellite during September 1962. The results tend to support a conclusion that strong signals and high absorptions are associated with no-cloud or low-cloud atmospheres, and weak signals with low absorption are associated with high-cloud atmospheres.

### References

- McGee, R. A., "An analytical infrared radiation model of the earth," *Appl. Opt.* **1**, 649-653 (September 1962).
- Good, L., "Earth background radiation analysis," General Electric Rept. R60ELC94 (December 1960).
- Altshuler, T. L., "Infrared transmission and background radiation by clear atmospheres," General Electric Rept. R61SD199 (December 1961).
- Proc. Inst. Radio Engrs. **47**, 1413-1700 (1959). (Special issue on Infrared Physics and Technology.)
- Block, L. C. and Lovett, J. J., "Infrared background spectral radiation measurements from on-board a Discoverer satellite," *Proc. Infrared Information Symposia* **8**, 1, 95-104 (January 1963).